Science Advances
AAAS

advances.sciencemag.org/cgi/content/full/5/12/eaay0764/DC1

Supplementary Materials for

Printing of wirelessly rechargeable solid-state supercapacitors for soft, smart contact lenses with continuous operations

Jihun Park, David B. Ahn, Joohee Kim, Eunkyung Cha, Byeong-Soo Bae, Sang-Young Lee*, Jang-Ung Park*

*Corresponding author. Email: jang-ung@yonsei.ac.kr (J.-U.P.); syleek@unist.ac.kr (S.-Y.L.)

Published 6 December 2019, *Sci. Adv.* **5**, eaay0764 (2019)
DOI: 10.1126/sciadv.aay0764

The PDF file includes:

Other Supplementary Material for this manuscript includes the following:

(available at advances.sciencemag.org/cgi/content/full/5/12/eaay0764/DC1)

Movie S1 (.avi format). Video clip showing the DIW-based dispensing procedure of the electrode ink on the smart contact lens substrate.
Movie S2 (.avi format). Video clip showing the DIW-based dispensing procedure of the electrolyte ink on top of the previously fabricated electrodes.

Movie S3 (.avi format). Video clip showing wireless the charging and discharging operation on the mannequin eye.
Movie S4 (.avi format). Video clip showing the heat generation test in the wearing of the soft, smart contact lens on the human eye.

Supplementary Materials

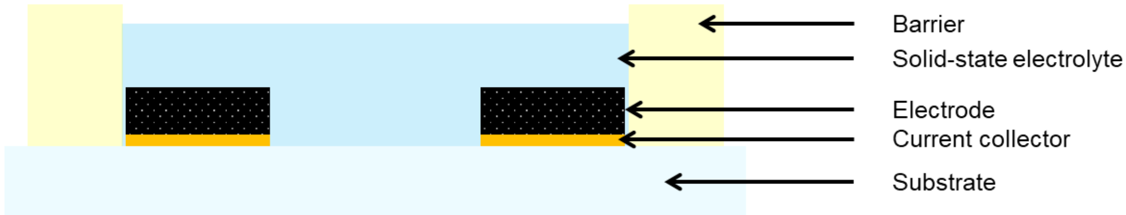

Fig. S1. The schematic layout of the printed supercapacitor.

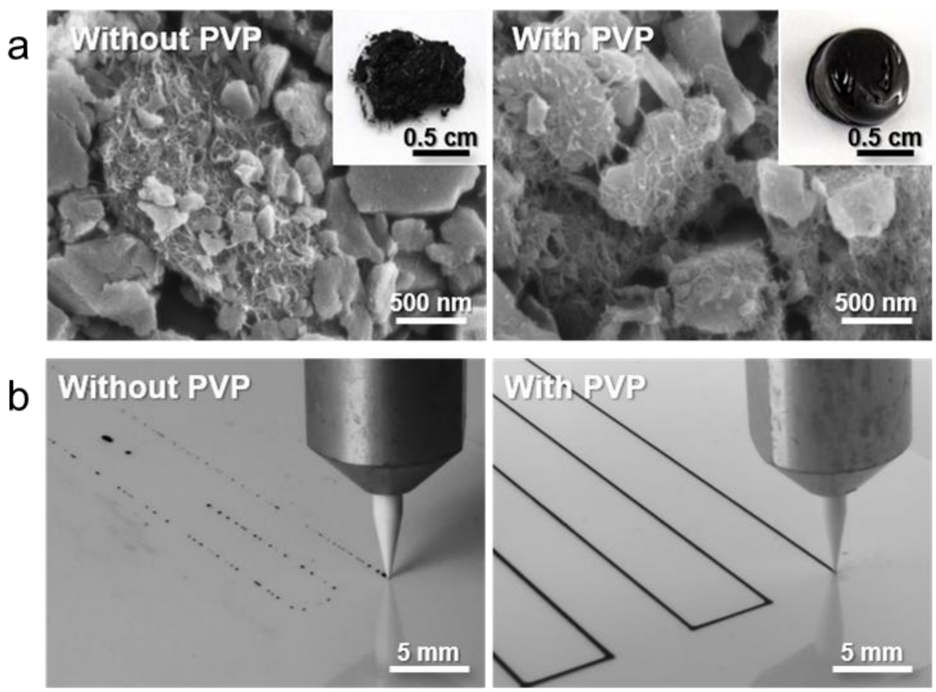

Fig. S2. Effect of PVP additive on electrode inks. a, Dispersion state (shown by SEM images and photographs (insets)) and **b**, dispensing stability through a micronozzle (diameter = 100 μm).

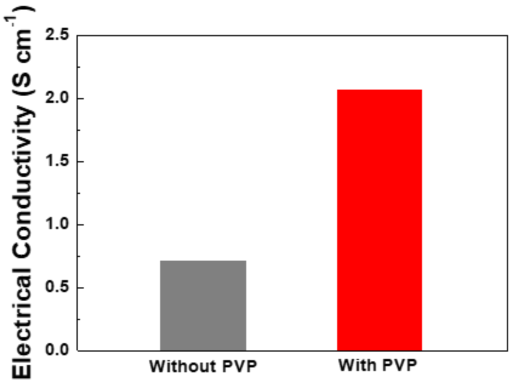

Fig. S3. Effect of PVP additive on electrical conductivity of the resulting electrodes (without PVP additive versus with PVP additive).

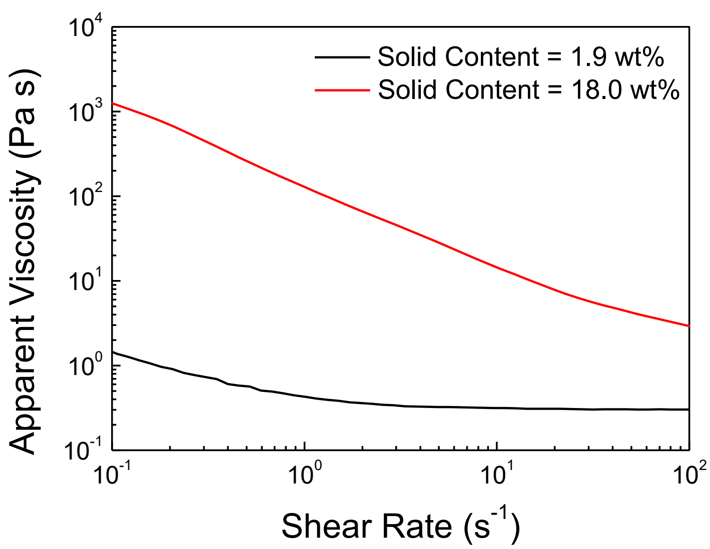

Fig. S4. Viscosity of the electrode inks (solid content, 1.9 and 18.0 wt %) as a function of shear rate.

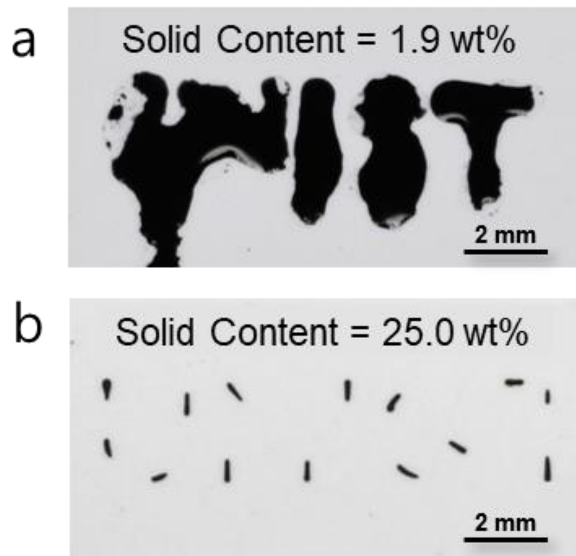

Fig. S5. Effect of solid content on electrode fabrication through DIW process. Photographs of the electrodes fabricated through the DIW process, in which solid content of the electrode ink: **a**, 1.9 wt% and **b**, 25.0 wt%.

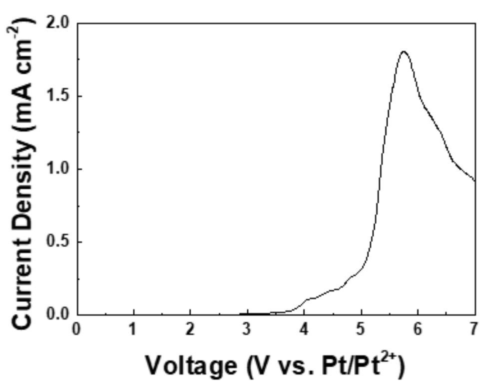

Fig. S6. LSV profiles of the solid-state polymer electrolyte (scan rate, 1.0 mV/s).

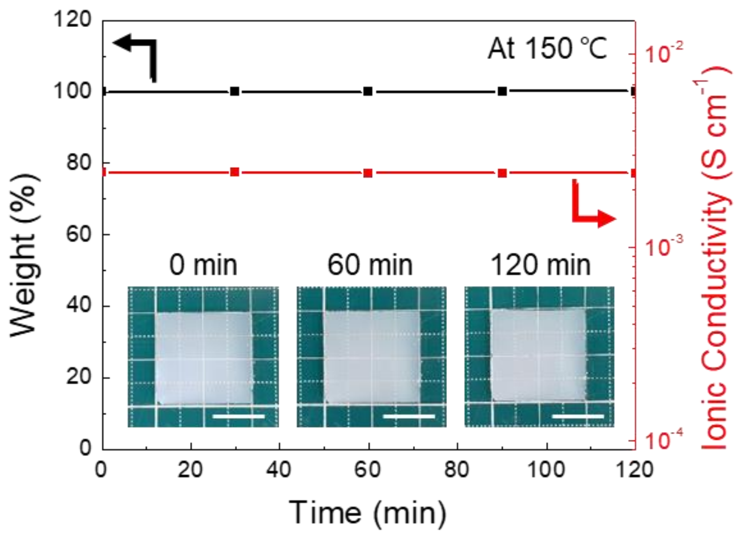

Fig. S7. Weight retention and ionic conductivity of the solid-state polymer electrolyte at 150°C as a function of time. The insets are photographs of the solid-state polymer electrolytes that had been at 150 °C for 0, 60, 120 minutes. Scale bars, 1 cm.

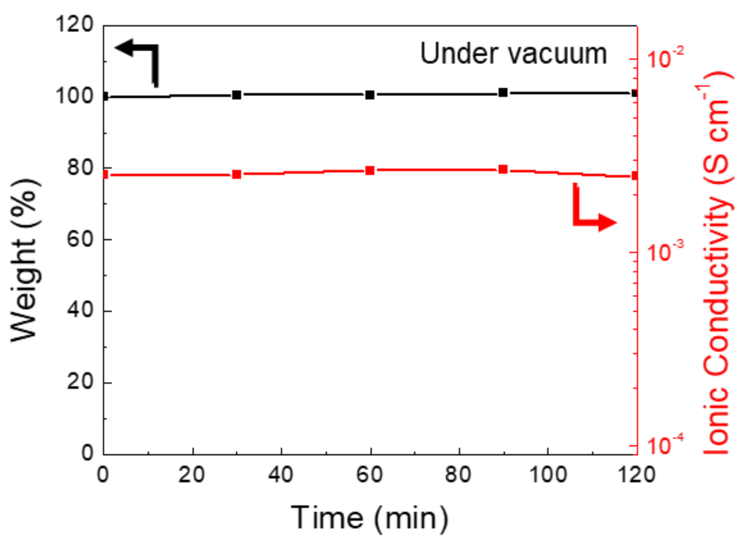

Fig. S8. Weight retention and ionic conductivity of the solid-state polymer electrolyte in a vacuum as a function of time.

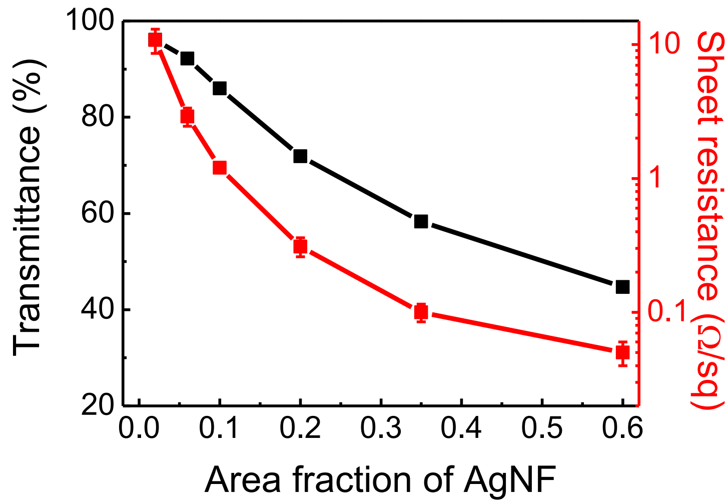

Fig. S9. Optical and electrical characteristics of AgNF-AgNW hybrid films. Sheet resistance and optical transmittance of the AgNF-AgNW hybrid films as a function of area fraction of AgNF.

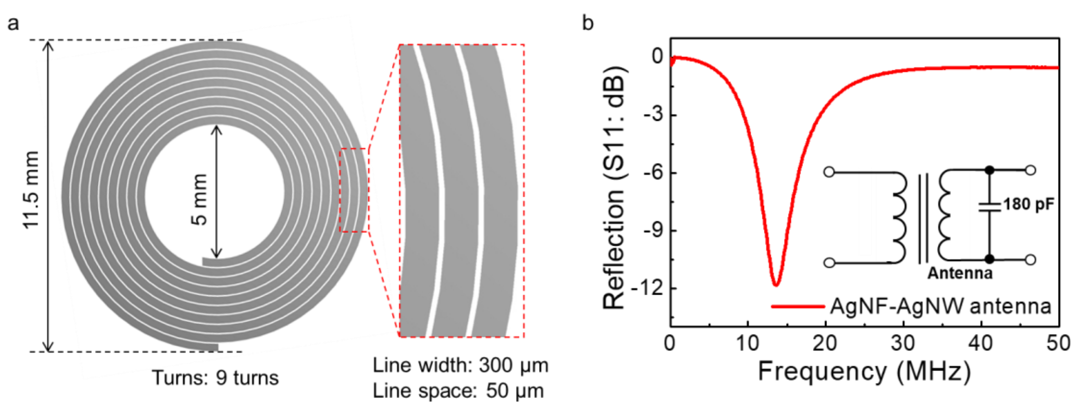

Fig. S10. Design and properties of the antenna for WPT. a, Design of antenna. **b**, Resonance properties of the antenna using AgNF-AgNW hybrid films.

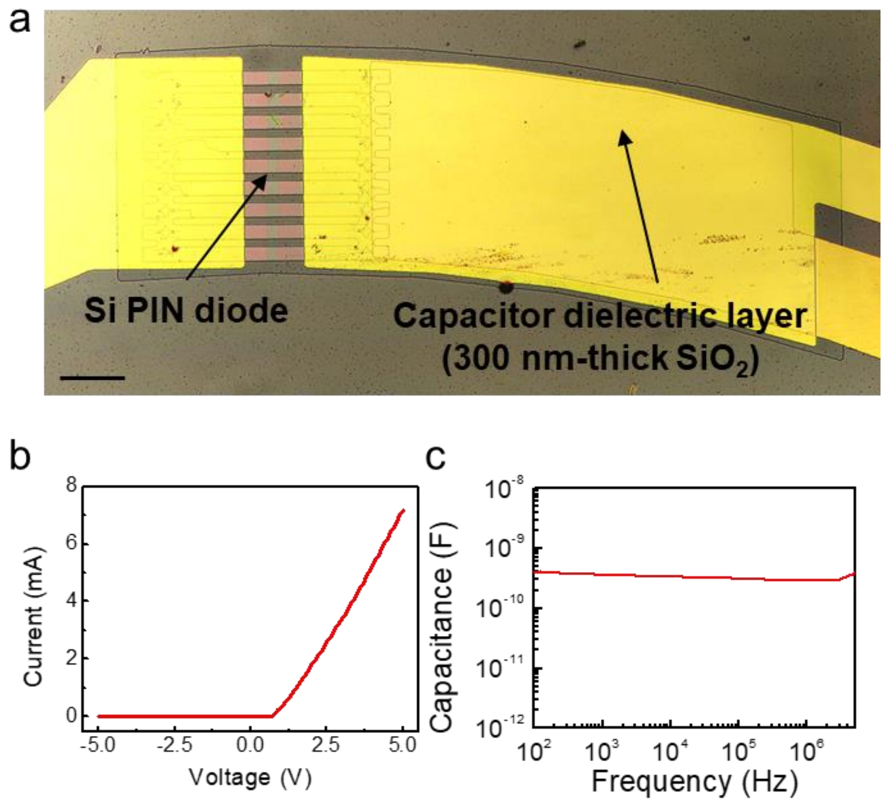

Fig. S11. Rectifier circuit based on Si PIN diodes and SiO_2-based capacitor. a, Optical photograph of rectifier. **b**, I-V curve of a single Si diode. **c**, Characteristics of SiO_2-based capacitor.

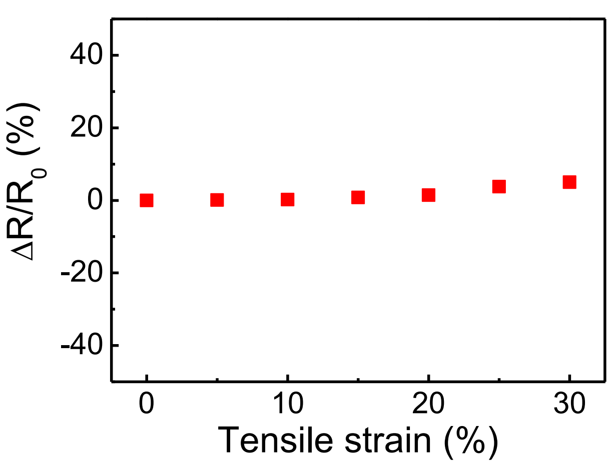

Fig. S12. Biaxially stretching tests of AgNF-AgNW hybrid films.

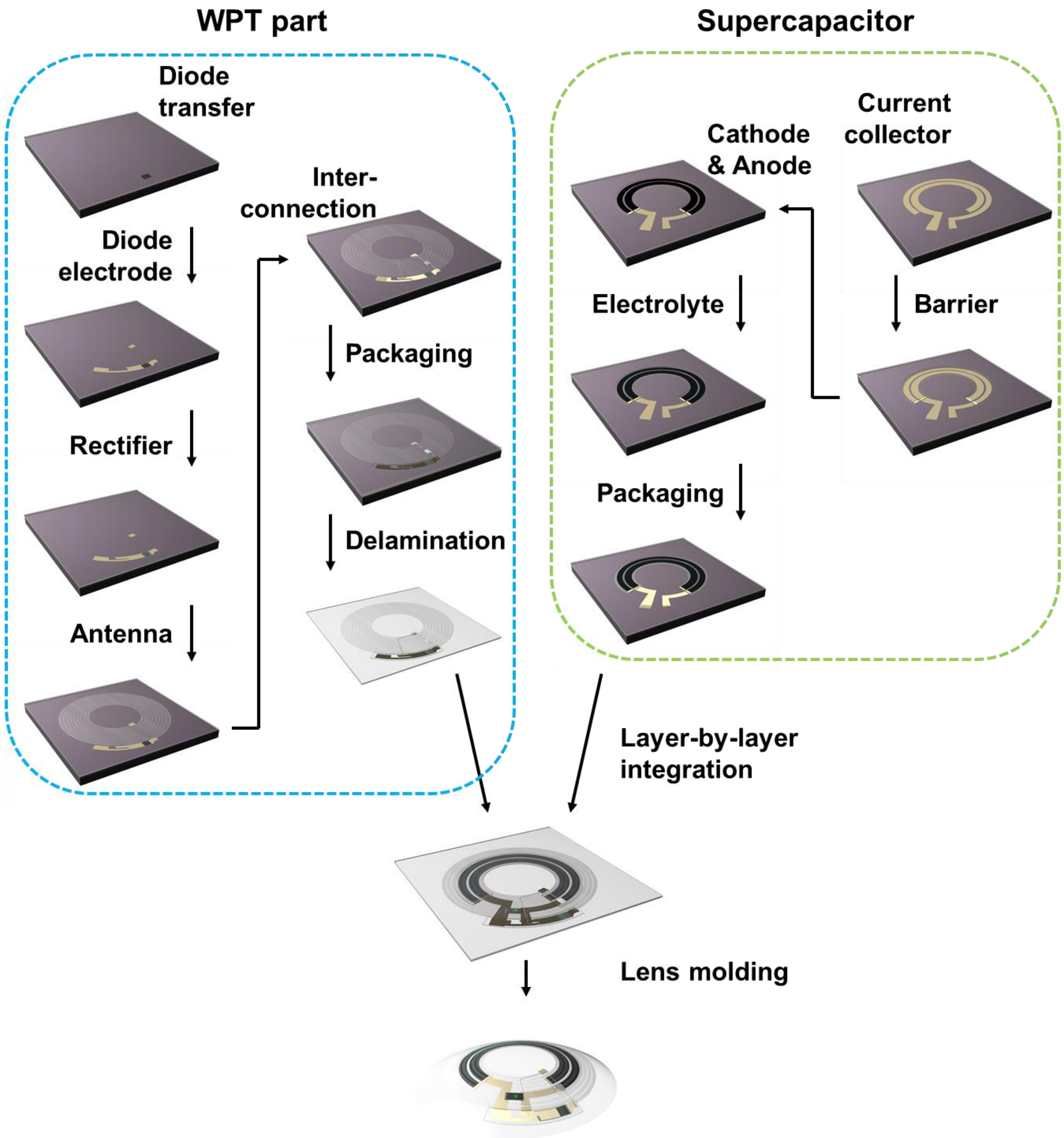

Fig. S13. Fabrication of a fully integrated soft, smart contact lens system.

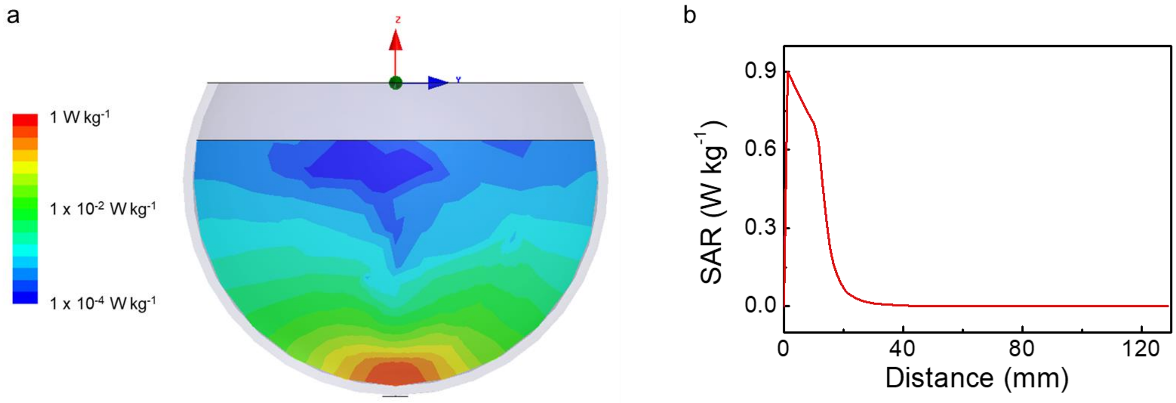

Fig. S14. SAR simulation results. a, SAR simulation distribution when the transmitting power sets as 10 W for the extreme environment. **b**, SAR simulation result as a function of distance.

Movie S1. Video clip showing the DIW-based dispensing procedure of the electrode ink on the smart contact lens substrate.

Movie S2. Video clip showing the DIW-based dispensing procedure of the electrolyte ink on top of the previously fabricated electrodes.

Movie S3. Video clip showing wireless the charging and discharging operation on the mannequin eye.

Movie S4. Video clip showing the heat generation test in the wearing of the soft, smart contact lens on the human eye.